

Characterization of (PEO)LiClO₄-Li_{1.3}Al_{0.3}Ti_{1.7}(PO₄)₃ Composite Polymer Electrolytes with Different Molecular Weights of PEO

Yan-Jie Wang,¹ Yi Pan,¹ Li Wang,¹ Ming-Jie Pang,¹ Linshen Chen²

¹Department of Materials Science and Engineering, Zhejiang University, Hangzhou 310027, People's Republic of China
²Center of Analysis and Measurement, Zhejiang University, Hangzhou 310027, People's Republic of China

Received 27 April 2005; accepted 15 November 2005

DOI 10.1002/app.24786

Published online in Wiley InterScience (www.interscience.wiley.com).

ABSTRACT: A group of polyethylene oxide (PEO)LiClO₄-Li_{1.3}Al_{0.3}Ti_{1.7}(PO₄)₃ composite polymer electrolyte (CPE) films was prepared by the solution-cast method. In each film, EO/Li = 8 and the Li_{1.3}Al_{0.3}Ti_{1.7}(PO₄)₃ content of 15 wt % were fixed, but the number averaged molecular weight of PEO (M_n) was altered from 5 to 7×10^4 to 10^6 , 2.2 – 2.7×10^6 , 3 – 4×10^6 , 4 – 5×10^6 , and 5.5 – 6×10^6 , respectively. Several techniques including X-ray diffraction (XRD), differential scanning calorimetry (DSC), scanning electron microscopy (SEM), and electrical impedance spectroscopy (EIS) were used to characterize the CPE films. LiClO₄ was found to have a strong tendency to complex with PEO, but Li_{1.3}Al_{0.3}Ti_{1.7}(PO₄)₃ was rather dispersed in PEO matrix. DSC analysis revealed that the amorphous phase was dominant in the CPE films although the PEOs before-use was considerably crystalline.

SEM study showed smooth and homogeneous morphologies of the films with low molecular weight PEO and a dual phase characteristic for those with high molecular weight PEO. EIS results indicated that the CPE films are all ionic conductor and the conducting behavior obeys Vogel-Tamman-Fulcher (VTF) equation. The parameters in VTF equation were obtained and discussed by taking into considerations PEO molecular weights and crystallinities of the CPE films. Of all the films, the one with PEO with the smallest $M_n = 5$ – 7×10^4 had the maximum conductivity, i.e., 1.590×10^{-5} S cm⁻¹ at room temperature and 1.886×10^{-3} S cm⁻¹ at 373 K. © 2006 Wiley Periodicals, Inc. *J Appl Polym Sci* 102: 4269–4275, 2006

Key words: polyethylene oxide; polymer electrolyte; conductivity

INTRODUCTION

In contrast to liquid electrolytes in lithium-ion batteries, solid electrolytes have attracted much attention because of their advantages over liquid electrolytes, such as ease of fabrication, low electrolyte leakage, safety and reliability in batteries.^{1–4} An ideal electrolyte for solid state lithium batteries should have not only high lithium-ion conductivity and large transport number but also a rubbery mechanical performance to accommodate electrode dimensions changes during charging and discharging. With such expectations, polyethylene oxide (PEO) doped with sodium salts was suggested earlier by Wright and coworkers,^{5,6} and was later recognized by Armand et al.,⁷ potentially applicable in high specific energy batteries and other electrochemical devices. PEO and other polymers such as polyacrylonitrile (PAN), polymethyl methacrylate (PMMA), polyvinylidene fluoride (PVdF), etc., which can form ionic complexes with metal salts of low lattice energy, particularly lithium salt,⁸ have been used as a polymer matrix of solid polymer electrolytes (SPE). It has been also

evident that lithium ionic transport mainly takes place in the amorphous phases, and that the conductivity in amorphous phase was two to three orders of magnitude higher than in the crystalline ones in SPE.^{9,10} Most research efforts, therefore, have been dedicated to obtain SPE films containing large amounts and stable amorphous phases to obtain a good flexibility of the polymer chains favoring the ion transport.

Ceramic powders, such as Al₂O₃, SiO₂, and Li₃N, may be added as fillers to improve the ionic conductivity but to preserve the mechanical strength and stability of the electrode/electrolyte interface.^{11–13} Instead of nonconducting oxides, fast ionic conductors (FIC), e.g., Li_{1.4}Al_{0.4}Ge_{1.7}(PO₄)₃ and 14Li₂O-9Al₂O₃-38TiO₂-39P₂O₅ used as fillers in the PEO-based CPE films and their positive effects on both mechanical properties and ionic conductivity were reported by Leo et al. and Zhang et al.^{14–16} Recently, Li_{1.3}Al_{0.3}Ti_{1.7}(PO₄)₃ filler effect on (PEO)LiClO₄ solid polymer electrolyte was reported by the authors.¹⁷ The (PEO)-LiClO₄-Li_{1.3}Al_{0.3}Ti_{1.7}(PO₄)₃ CPE films with overall EO/Li = 8 and 15 wt % Li_{1.3}Al_{0.3}Ti_{1.7}(PO₄)₃ had the optimum ionic conductivity, i.e., 1.387×10^{-5} S/cm at room temperature and 1.378×10^{-5} S/cm at 373 K.¹⁷ This work extends the study to the investigation of (PEO)LiClO₄-Li_{1.3}Al_{0.3}Ti_{1.7}(PO₄)₃ CPE films with overall EO/Li = 8 and 15 wt % Li_{1.3}Al_{0.3}Ti_{1.7}(PO₄)₃

Correspondence to: Y.-J. Wang (yip@zju.edu.cn).

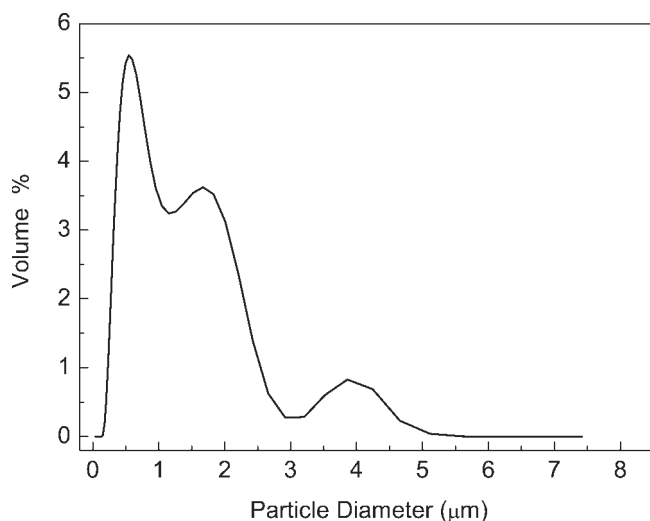


Figure 1 Particle size distribution of the $\text{Li}_{1.3}\text{Al}_{0.3}\text{Ti}_{1.7}(\text{PO}_4)_3$ salt after ball milling.

but different molecular weight of PEO. The films preparation, their phase composition, thermal behavior, morphologies, and ionic conductivities are studied. The effects of PEO molecular weight on all those mentioned earlier were discussed.

EXPERIMENTAL

Synthesis of materials

The preparation of $\text{Li}_{1.3}\text{Al}_{0.3}\text{Ti}_{1.7}(\text{PO}_4)_3$ made from raw materials Li_2CO_3 , Al_2O_3 , TiO_2 , and $(\text{NH}_4)_2\text{HPO}_4$ was based on the method described by Aono et al.¹⁸ Before using, the $\text{Li}_{1.3}\text{Al}_{0.3}\text{Ti}_{1.7}(\text{PO}_4)_3$ ceramic confirmed by X-ray diffraction was proved to be an air-stable lithium ion conductor of about 10^{-4} S/cm at room temperature. The ceramic was crashed and

milled using agate balls in alcohol for 90 h to reach the particle size distribution (Fig. 1), which has been thought satisfactory to be incorporated into PEO matrix for this study.¹⁵ The fine powder was dried in vacuum at 120°C for 48 h to get rid of all possibly attached water molecules.

The PEO polymers with the number average molecular weights, $M_n = 5\text{--}7 \times 10^4$ (M_1), 10^6 (M_2), $2.2\text{--}2.7 \times 10^6$ (M_3), $3\text{--}4 \times 10^6$ (M_4), $4\text{--}5 \times 10^6$ (M_5), and $5.5\text{--}6 \times 10^6$ (M_6) supplied by Aldrich Chemicals were solely dried in vacuum at 50°C for 48 h right before the preparation of CPE films. Acetonitrile (reagent grade) used as the solvent was doubly distilled and stored over 4 Å molecular sieves prior to use. Anhydrous LiClO_4 provided by Zhangjiangang Guotai-Huarong New Chemical Materials, China, was used as main lithium ion contributor in CPE after dried at 120°C for 24 h.

$\text{Li}_{1.3}\text{Al}_{0.3}\text{Ti}_{1.7}(\text{PO}_4)_3$, LiClO_4 , and one of the PEO powders were appropriately weighed to guarantee the $\text{Li}_{1.3}\text{Al}_{0.3}\text{Ti}_{1.7}(\text{PO}_4)_3$ content of 15 wt % and $\text{EO}/\text{Li} = 8$ in each CPE system, and then introduced to the above treated acetonitrile in a beaker followed by stirring at $50\text{--}70^\circ\text{C}$ until a homogenous suspension was formed. The suspension was cast onto a Teflon plate, and then slowly dried at room temperature. The final films with the thickness of $150\text{--}300$ μm were yielded and dried at $45\text{--}50^\circ\text{C}$ in vacuum for 24 h before measurements. Corresponding to each PEO used, the films were labeled by CPE(1), CPE(2), CPE(3), CPE(4), CPE(5), and CPE(6), respectively.

Characterization

The phases of various pure PEOs and CPE films were analyzed in XRD (Bruker-AXS, 30 kV, Cu Kα radiation with a step width of 0.02°) at room temper-

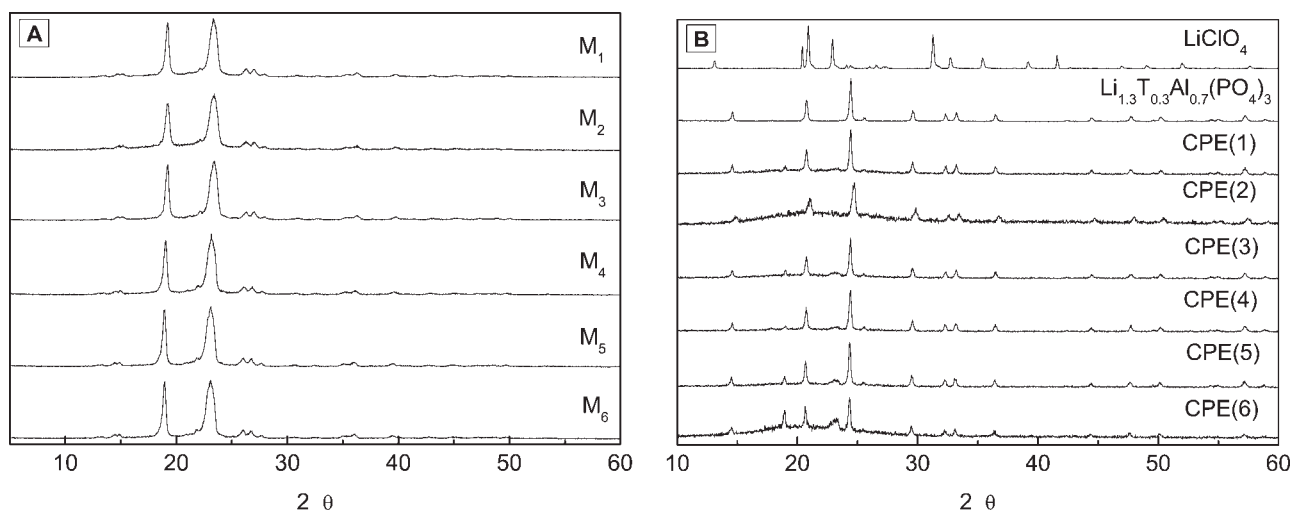


Figure 2 X-ray diffraction patterns at room temperature of (A) pure PEO with different molecular weight and (B) LiClO_4 and $\text{Li}_{1.3}\text{Al}_{0.3}\text{Ti}_{1.7}(\text{PO}_4)_3$ and the different CPE films with fixed $\text{EO}/\text{Li} = 8$ and 15 wt % $\text{Li}_{1.3}\text{Al}_{0.3}\text{Ti}_{1.7}(\text{PO}_4)_3$.

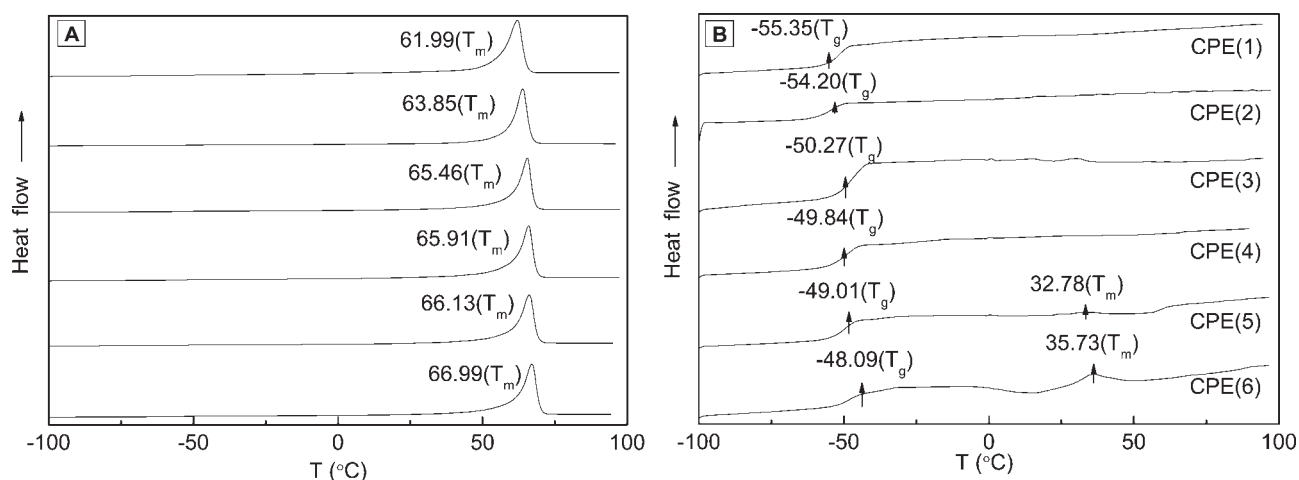


Figure 3 DSC curves of the PEOs with different molecular weights and the CPE films made from these PEO with fixed EO/Li = 8 and 15 wt % Li_{1.3}Al_{0.3}Ti_{1.7}(PO₄)₃ content.

ature. The thermographs over -100 to 100°C of the films were obtained using DSC (Q100 V7.3 Build 249 Instruments) with liquid nitrogen-cooled heating element. Each sample to be analyzed on the DSC was sealed in aluminum pans, and was first heated from 25 to 100°C , and then cooled to -100°C and started to be measured by heating again to 100°C at a heating rate of $10^{\circ}\text{C}/\text{min}$. Morphology observation of the films was carried out in SEM (Hitachi S-570). Thin electrolyte films prepared by a solution-cast technique were mounted onto 1 cm diameter aluminum plates. Samples were sputter-graphite-coated (20 nm). The surface morphology of all specimens was examined at a working voltage of 25 KV. The ionic conductivity was determined using electrical impedance spectrum (EIS) method at some different temperatures. The CPE film samples were sandwiched between stainless steel blocking electrodes and placed in a temperature-controlled furnace. The impedance of the films was measured using the frequency response analyzer (FRA Solartron model 1255) with a Solartron model 1287 electrochemical interface over the frequency range from 1 Hz to 1 MHz.

RESULTS AND DISCUSSION

Phases

Figure 2(A,B) show the XRD patterns of various pure PEOs, two lithium salts and the CPE films. In Figure 2(A), two strong peaks at $2\theta = 19.5^{\circ}$ and 23.5° and minor peaks at 15.08° , 26.24° , 26.94° , 35.3° , 36.26° , and 39.68° are found at all PEOs, suggesting that all the PEOs are intrinsically crystalline polymers with high crystallinity. Additionally, the X-ray traces of the CPE films in Figure 2(B) explicitly show that LiClO₄ characteristic peaks at 13.16° , 20.38° , 20.88° , 22.9° , 31.24° , 39.14° , 41.56° , 47° , 49.04° , and

52.04° disappear, and that Li_{1.3}Al_{0.3}Ti_{1.7}(PO₄)₃ characteristic peaks at 14.54° , 20.76° , 24.4° , 25.54° , 29.52° , 32.36° , 33.26° , 36.46° , 44.52° , 47.72° , 50.26° , 55.06° , 57.26° , and 58.9° remain, indicating LiClO₄ was dissolved, i.e., complexed with PEO and Li_{1.3}Al_{0.3}Ti_{1.7}(PO₄)₃ was mechanically dispersed rather than complexed in PEO, the previous of which is in agreement with the work done by Robitaille and Fauteux¹⁹ and Vallée et al.²⁰ Meanwhile, the intensities of two main peaks of pure PEO in CPE films slightly decreases with the decrease in molecular weight of PEO, suggesting that the degree of crystallinity of PEO in the CPE films is low as the molecular weight is low. This will be further discussed in the following section.

Crystallinity

The DSC thermograms obtained from pure PEOs and the CPE films are drawn in Figure 3(A,B), respectively. For pure PEOs, only melting peaks and consequently melting temperature (T_m) are identifiable. For CPE films, however, the glass transition temperatures can be determined, but the melting peaks do not show up except for CPE(5) and CPE(6). The

TABLE I
Thermal Properties of PEO with Different Molecular Weight and the CPE Films

PEO	T_0 (K)	A ($\text{S cm}^{-1} \text{K}^{1/2}$)	E_a (eV)
M ₁	187.65	61.671	0.135
M ₂	188.8	40.280	0.132
M ₃	192.73	28.278	0.125
M ₄	193.16	18.853	0.123
M ₅	193.99	16.280	0.122
M ₆	194.91	14.410	0.121

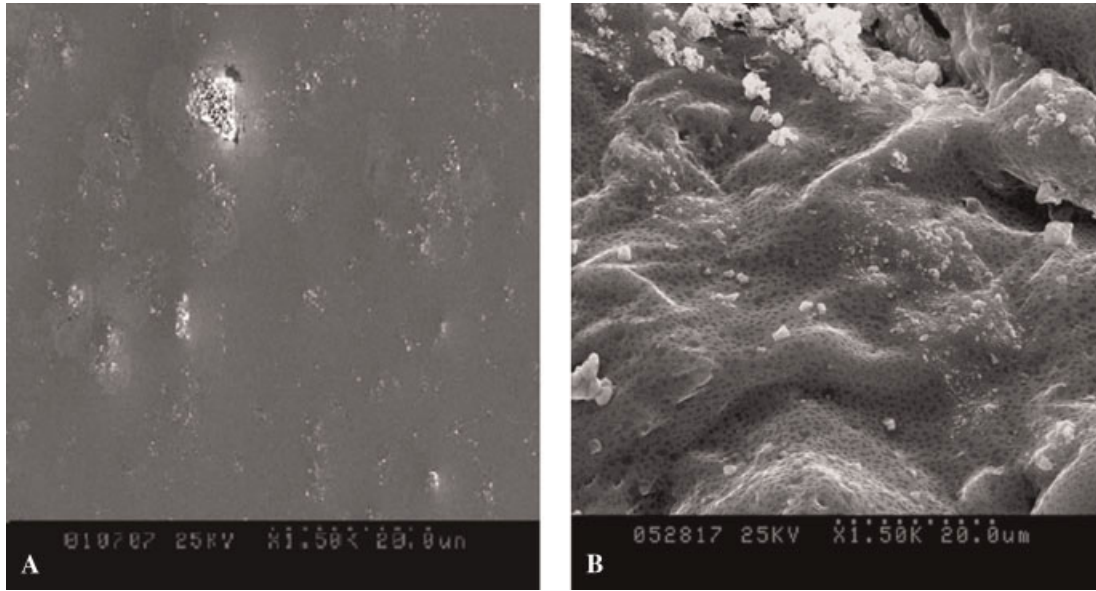


Figure 4 SEM micrographs of the CPE films with different molecular weight of PEO: (A) CPE (1); (B) CPE (6).

possibly defined T_g and T_m are marked on Figure 3 and summarized in Table I. It is suggested that the addition of two lithium salts inhibited the crystallization of PEO in CPE films so that low molecular weight CPE(1–4) did not give melting peaks and high molecular weight CPE(5–6) gave faded melting peaks. The inhibition of crystallization may favor the lithium ionic conductivity since the ionic transport only takes place in the amorphous region of CPE.^{9,10} On the basis of these curves, the crystallinities (χ_c) of them are calculated using the following equations:

$$\chi_c(\text{CPE}) = \frac{\Delta H_{m,\text{CPE}}}{\Delta H_{m,\text{CPE}}^0} \quad (1)$$

$$\chi_c(\text{PEO}) = \frac{\Delta H_{m,\text{PEO}}}{\Delta H_{m,\text{PEO}}^0} \quad (2)$$

where $\Delta H_{m,\text{CPE}}$ and $\Delta H_{m,\text{PEO}}$ are the apparent melting enthalpies per gram of CPE and PEO present in the CPE, respectively, and $\Delta H_{m,\text{PEO}}^0$ is the heat of melting per gram of 100% crystalline PEO. T_g and T_m of the pure PEOs and the CPE films as well as their $\Delta H_{m,\text{PEO}}^0$ and $\Delta H_{m,\text{PEO}}$ ^{21,22} and χ_c are also summarized in Table I. It is seen in Table I that the crystallinities of pure PEOs fluctuate around 63 to 74%, but those of CPE are mostly at zero and 0.425% and 2.26% for CPE(5) and CPE(6), respectively. Besides that, T_m for CPE(5) and CPE(6), only which have well defined T_m , are much lower than pure PEO.

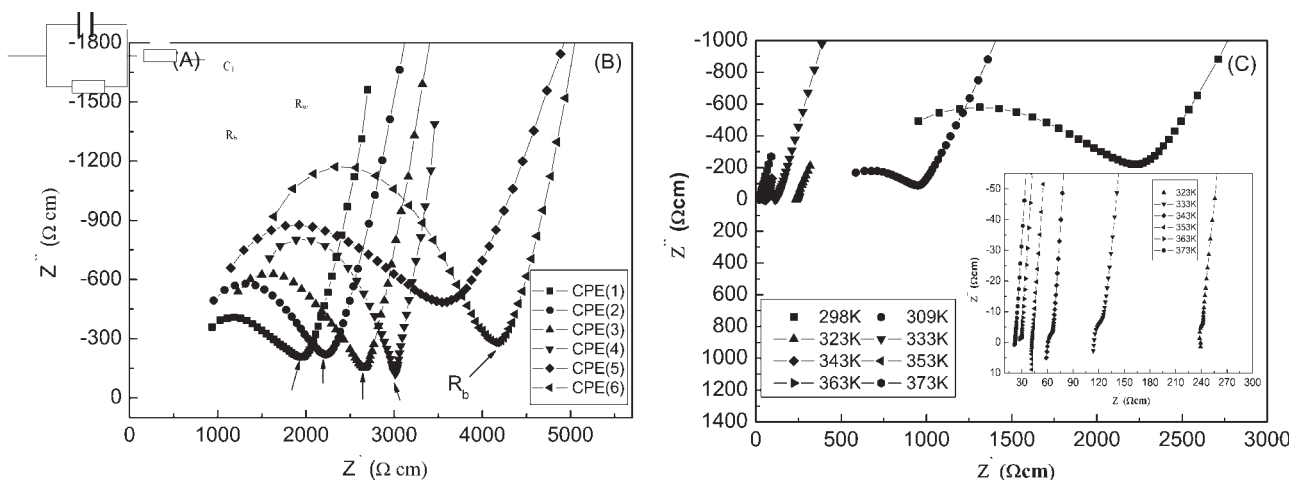


Figure 5 (A) Equivalent circuit for the simulation of impedance spectra. (B) The impedance spectra of the CPE films at room temperature with different molecular weight. (C) The impedance spectra of the CPE(2) films at varied temperatures.

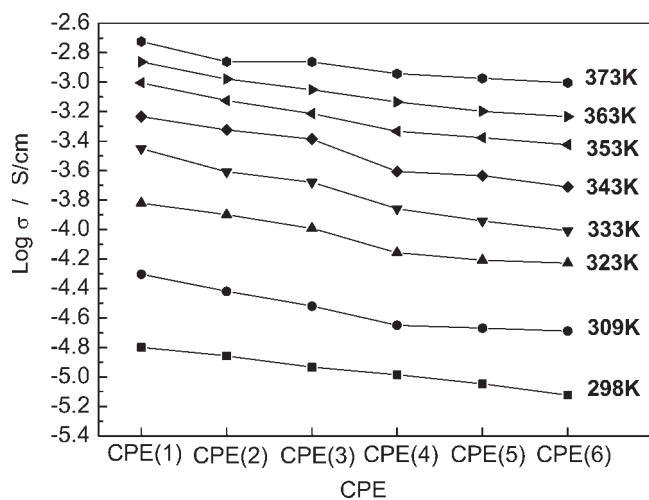


Figure 6 Ionic conductivities as a function of molecular weight for the CPE films at various temperatures.

Morphology

The surfaces of all CPE films, which were only PEO envelopes, were observed in SEM, but only the surface morphologies of CPE(1) and CPE(6) are shown in Figure 4(A,B), representing completely amorphous and partial crystalline PEO in the films. The surface of CPE(1) is smooth, but CPE(6) exhibits dual phase characteristic, confirming the DSC results that high molecular weight PEO in CPE film is partially crystalline.

Electrical impedance spectra

The electrical impedance spectra of CPE films were measured at various temperatures. The room temperature impedance spectra of the CPE films with different PEO molecular weights are shown in Figure 5(B). The use of ac techniques for classical

electrochemical measurements has been reviewed by Armstrong et al.,²³ but the problem of surface roughness has been ignored. The spectra of each film situated between two stainless steel (SS) electrodes are all consist of a depressed semicircle in high frequency range and a straight line in low frequency range. The former represents the ionic impedance of the polymer electrolyte, and the straight line is from the stainless steel electrodes and can be attributed to the ion diffusion in the polymer electrolyte. The semicircle part of each spectrum can be modeled using an equivalent circuit in Figure 5(A). The physical meanings of the elements in this assumed equivalent circuit are as follows: R_b and C_1 represent the bulk resistance and the geometrical capacitance of the electrolyte respectively; R_w represents the Warburg impedance. The equivalent circuit is commonly used in the analysis of impedance spectroscopy because it is simple and can provide a complete picture of the system.²⁴ Using this equivalent circuit, R_b , C_1 , and R_w can be estimated by superimposing the best fit to the measured spectrum are shown in Figure 5(B).

The impedance spectra of the CPE(2) films at different temperatures are shown in Figure 5(C). At higher temperatures (≥ 323 K), the semicircle shrinks as a result of its shift to higher frequencies due to the decrease of the ionic resistance of the polymer electrolyte. In this case, R_b was determined using the intercepting point of the inclined line with Z' axis.

The ionic conductivity is calculated by

$$\sigma = \frac{d}{R_b A} \quad (3)$$

where d and A represent the thickness and the area of the sample, respectively. The conductivity of CPE film with fixed EO/Li = 8 and 15 wt % Li_{1.3}Al_{0.3}Ti_{1.7}(PO₄)₃ at different temperatures are plotted against

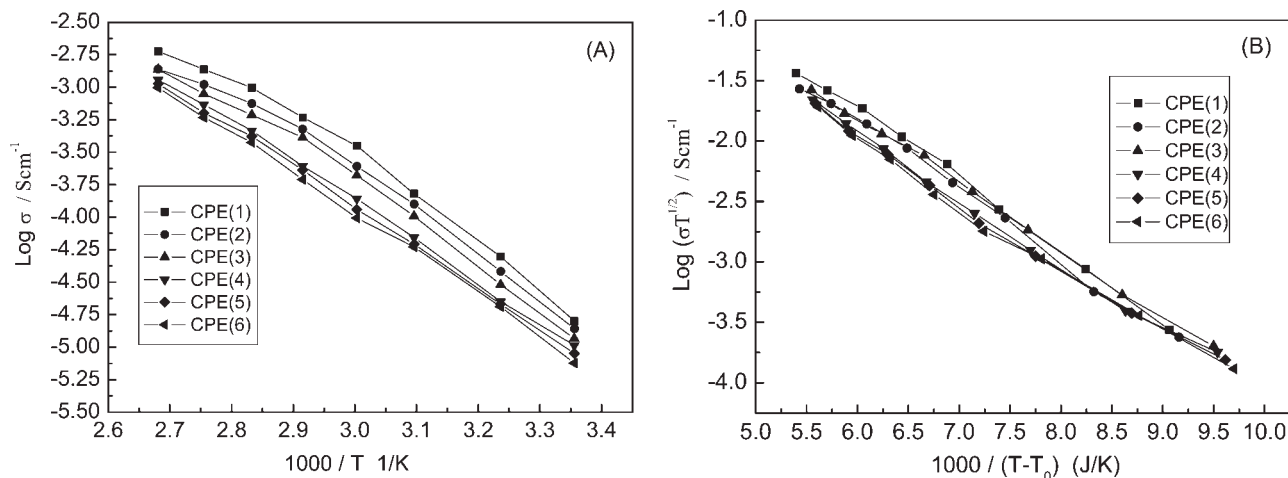


Figure 7 Temperature dependent conductivity of the CPE films with fixed EO/Li = 8 and various molecular weight PEO but 15 wt % Li_{1.3}Al_{0.3}Ti_{1.7}(PO₄)₃ content.

TABLE II
Fitted Parameters Obtained from Conductivity Data for the CPE Films

PEO and CPE	T_g (°C)	T_m (°C)	ΔH_m (J/g)	ΔH_{PEO}^0 (J/g)	χ_c (%)
M ₁	–	61.99	129.3	182.52	46.92
M ₂	–	63.85	129.7	188.00	68.99
M ₃	–	65.46	129.8	192.74	67.34
M ₄	–	65.91	131.5	194.07	67.76
M ₅	–	66.13	136.1	194.71	69.90
M ₆	–	66.99	145.0	197.25	73.51
CPE(1)	–55.35	–	–	182.52	–
CPE(2)	–54.20	–	–	188.00	–
CPE(3)	–50.27	–	–	192.74	–
CPE(4)	–49.84	–	–	194.07	–
CPE(5)	–49.01	32.78	0.827	194.71	0.425
CPE(6)	–48.09	35.73	4.450	197.25	2.256

PEO molecular weight in Figure 6. For the CPE films, when the temperature increases, the ionic conductivity mainly increases because the crystallinity is severely damaged after the addition of $\text{Li}_{1.3}\text{Al}_{0.3}\text{Ti}_{1.7}(\text{PO}_4)_3$ and LiClO_4 to PEO. After temperature increases above T_m , the disappearance of crystalline phase and consequently the increase of amorphous regions in the CPE films make ionic conductivity high. For the CPE(1–4) films, the increase of ionic conductivity with increasing temperature is attributed to higher and higher ionic mobility in amorphous phase because there are no T_m as shown in DSC studies. Additionally, the ionic conductivity of the film is low as the molecular weight of PEO in the film is high. CPE(1) with the smallest molecular weight has the highest conductivity, i.e., $1.590 \times 10^{-5} \text{ S cm}^{-1}$ at room temperature and $1.886 \times 10^{-3} \text{ S cm}^{-1}$ at 373 K.

To further study the temperature dependence of the conductivity, two plots are drawn in Figures 7(A) and 7(B), respectively. One is $\log \sigma$ vs. $1000/T$ and another is $\log \sigma T^{-0.5}$ vs. $1000/T$, corresponding to Arrhenius relationship and Vogel-Tammann-Fulcher (VTF) equation^{25–27} i.e., eq. (4), respectively.

$$\sigma = AT^{-1/2} \exp[-E_a/k_B(T - T_0)] \quad (4)$$

where k_B is the Boltzman constant, T_0 is a reference temperature, which is usually 30–50 K lower than T_g .^{28–30} It can be seen that VTF equation fits better than the Arrhenius relationship, and is thus adopted to describe the ionic conduction behavior of the CPE films in this study.

By fitting the conductivity data to eq. (4), T_0 , A , and E_a were obtained and are summarized in Table II. The VTF equation applied to polymer electrolytes has been discussed by Berthier et al.⁹ The preexponential factor, A , is proportional to the number of ionic charge carriers. The pseudoactivation energy E_a reflects the energy characteristics combining various

ion–polymer and ion–ion interactions, and is controlled by many factors, such as lattice energy of the salt, complexation degree, concentration, crystallinity, dielectric constant, etc. In Table II, A decreases while T_0 increases, but E_a does not change much with increasing molecular weight of PEO. These suggest that the number of ionic charge carriers reduces, the PEO matrix becomes less flexible, but the ion–polymer and ion–ion interactions are basically the same with the increase in PEO molecular weight.

CONCLUSIONS

As composite polymer electrolytes, (PEO) LiClO_4 - $\text{Li}_{1.3}\text{Al}_{0.3}\text{Ti}_{1.7}(\text{PO}_4)_3$ (15 wt % $\text{Li}_{1.3}\text{Al}_{0.3}\text{Ti}_{1.7}(\text{PO}_4)_3$ and $\text{EO/Li} = 8$) films with the number averaged molecular weights of PEO of $5\text{--}7 \times 10^4$, 10^6 , $2.2\text{--}2.7 \times 10^6$, $3\text{--}4 \times 10^6$, $4\text{--}5 \times 10^6$, and $5.5\text{--}6 \times 10^6$, respectively, can be successfully prepared using solution-cast technique. XRD study suggest that PEO matrix was largely complexed with LiClO_4 rather than $\text{Li}_{1.3}\text{Al}_{0.3}\text{Ti}_{1.7}(\text{PO}_4)_3$. DSC results indicate that the amorphous PEO with LiClO_4 complexed dominates in these CPE films after the addition of LiClO_4 and $\text{Li}_{1.3}\text{Al}_{0.3}\text{Ti}_{1.7}(\text{PO}_4)_3$ although the PEO-used are highly crystalline. The PEO enveloped surfaces observed in SEM exhibited smooth and homogeneous morphologies for the films with relatively low molecular weight of PEO and a dual phase (amorphous and crystalline) characteristics with high molecular weight. The analysis of EIS evidences that the ionic conductivity of CPE film is low as the molecular weight of PEO in the film is high. The conductivity of the film with PEO of $M_n = 5\text{--}7 \times 10^4$, the smallest in this study, is $1.590 \times 10^{-5} \text{ S cm}^{-1}$ at room temperature and $1.886 \times 10^{-3} \text{ S cm}^{-1}$ at 373 K. The ionic conducting behavior of the CPE films obeys VTF equation, which is

$$\sigma = AT^{-1/2} \exp[-E_a/k_B(T - T_0)]$$

A decreases while T_0 increases, but E_a does not change much with increasing molecular weight of PEO.

References

- Jacob, M. M. E.; Hackett, E.; Giannelis, E. P. *J Mater Chem* 2003, 13, 1.
- Bruce, P. G. *Electrochim Acta* 1995, 40, 2077.
- Armand, M.; Sanchez, J. Y.; Gauthier, M.; Choquette, Y. In *Electrochemistry of Novel Materials*; Lipkowski, J.; Ross, P. N. L., Eds.; VCH: New York, 1994; p 65.
- Quartarone, E.; Mustarelli, P.; Magistris, A. *Solid State Ionics* 1998, 110, 1.
- Fenton, D. E.; Parker, J. M.; Wright, P. V. *Polymer* 1973, 14, 589.
- Wright, P. V. *Br Polym J* 1975, 7, 319.
- Armand, M. B.; Chabagno, J. M.; Duclot, M. In *Fast Ion Transport in Solids*; Vashishta, P.; Mundy, J. N.; Shenoy, G. K., Eds.; Elsevier: New York, 1979; p 131.

8. Gray, F. M. *Solid Polymer Electrolytes*; VCH: New York, 1991.
9. Berthier, C.; Gorecki, W.; Minier, M.; Armand, M. B.; Chabagno, J. M.; Rigaud, P. *Solid State Ionics* 1983, 11, 91.
10. Stainer, M.; Hardy, L. C.; Whitmore, D. H.; Shriver, D. F. *J Electrochem Soc* 1984, 131, 784.
11. Tambelli, C. C.; Bloise, A. C.; Rosario, A. V.; Pereira, E. C.; Magon, C. J.; Donoso, J. P. *Electrochim Acta* 2002, 47, 1677.
12. Capiglia, C.; Mustarelli, P.; Quartarone, E.; Tomasi, C.; Magistris, A. *Solid State Ionics* 1999, 118, 73.
13. Skaarup, S.; West, K.; Julian, P. M.; Thomas, D. M. *Solid State Ionics* 1990, 40/41, 1021.
14. Leo, C. J.; Subba Rao, G. V.; Chowdari, B. V. R. *Solid State Ionics* 2002, 148, 159.
15. Leo, C. J.; Thakur, A. K.; Subba Rao, G. V.; Chowdari, B. V. R. *J Power Sourc* 2003, 115, 295.
16. Zhang, X.-W.; Wang, C. S.; Appleby, A. J.; Little, F. E. *J Power Sourc* 2002, 112, 209.
17. Wang, Y.-J.; Pan, Y. *J Polym Sci Part B: Polym Phys* 2005, 43, 743.
18. Aono, H.; Sugimoto, E.; Sadaoka, Y.; Imanaka, N.; Adachi, G. Y. *J Electrochem Soc* 1990, 137, 1023.
19. Robitaille, C. D.; Fauteux, D. *J Electrochem Soc* 1986, 133, 315.
20. Vallée, A.; Besner, S.; Homme, P. *J Electrochim Acta* 1992, 37, 1579.
21. Cimmino, S. *Makromol Chem* 1990, 19, 2447.
22. Rocco, A. M.; Da Fonseca, C. P.; Pereira, R. P. *Polymer* 2002, 43, 3601.
23. Armstrong, R. D.; Bell, M. F.; Metcalfe, A. A. *Electrochim Acta* 1976, 21, 98.
24. Han, D. G.; Choi, G. M. *Solid State Ionics* 1998, 106, 71.
25. Vogel, H. *Phys Z* 1922, 22, 645.
26. Tamman, G.; Hesse, W. *Z Anorg Allg Chem* 1956, 156, 245.
27. Fulcher, G. S. *J Am Ceram Soc* 1925, 8, 339.
28. Li, X.; Hsu, S. L. *J Polym Sci Polym Phys Ed* 1984, 22, 1331.
29. Bruce, P. G.; Vincent, C. A. *J Chem Soc Faraday Trans* 1993, 89, 3187.
30. Albinsson, I.; Mellander, B.-E.; Stevens, J. R. *J Chem Phys* 1992, 96, 681.